Reactive Fluorescence Turn-On Probes for Fluoride Ions in Purely Aqueous Media Fabricated from Functionalized Responsive Block Copolymers

ARTICLE *in* MACROMOLECULES · OCTOBER 2011

Impact Factor: 5.8 · DOI: 10.1021/ma2018588

Macromolecules

ARTICLE

pubs.acs.org/Macromolecules

Reactive Fluorescence Turn-On Probes for Fluoride Ions in Purely Aqueous Media Fabricated from Functionalized Responsive Block Copolymers

Yanyan Jiang,[†] Xianglong Hu,[†] Jinming Hu,[†] Hao Liu,[†] Hui Zhong,[*,‡] and Shiyong Liu[*,†]

[†]CAS Key Laboratory of Soft Matter Chemistry, Department of Polymer Science and Engineering, Hefei National Laboratory for Physical Sciences at the Microscale, University of Science and Technology of China, Hefei, Anhui 230026, China

[‡]School of Chemistry and Chemical Engineering, Huaiyin Normal University, Huaiyin, Jiangsu 223300, China

Supporting Information

ABSTRACT: We report on the fabrication of a novel type of responsive double hydrophilic block copolymer (DHBC)-based highly selective and sensitive fluorescence "turn-on" reactive probes for fluoride ions (F^-) working in purely aqueous media by exploiting F^--induced cyclization reaction of nonfluorescent moieties to induce the formation of fluorescent coumarin moieties, as inspired by the previous work of the Swager research group (Angew. Chem. Int. Ed. 2003, 42, 4803). Diblock copolymers bearing F^--reactive moieties (SiCouMA) in the thermoresponsive block, PEO-*b*-P(MEO_2MA-*co*-OEGMA-*co*-SiCouMA), were synthesized at first via reversible addition−fragmentation chain transfer (RAFT) technique followed by postmodification, where PEO, MEO_2MA, and OEGMA are poly(ethylene glycol), di(ethylene glycol) monomethyl ether methacrylate, and oligo(ethylene glycol) monomethyl ether methacrylate, respectively. As-synthesized diblock copolymers molecularly dissolve in water at room temperature and self-assemble into micellar nanoparticles above the critical micellization temperature (33 °C). In the presence of F^- ions, deprotection of nonfluorescent SiCouMA moieties followed by spontaneous cyclization reaction leads to the formation of highly fluorescent coumarin residues (CouMA). Thus, PEO-*b*-P(MEO_2MA-*co*-OEGMA-*co*-SiCouMA) diblock copolymers can serve as highly efficient and selective fluorescence "turn-on" reaction probes for F^- ions in aqueous media. In the range of 0−1600 equiv of F^- ions, diblock unimers and micellar solutions at 20 and 40 °C exhibit ~88-fold and ~30-fold increase in fluorescence emission intensity (20 min incubation time), respectively. The detection limits were determined to be 0.065 and 0.05 ppm for diblock unimers and micelles, respectively. Most importantly, in the low F^- concentration range, excellent linear correlation between F^- concentration and emission intensity was observed (0−15 ppm for unimers at 20 °C and 0−8 ppm for micelles at 40 °C). Interestingly, upon complete transformation of nonfluorescent SiCouMA moieties into fluorescent CouMA, the emission intensity of diblock copolymer solution decreases linearly with temperatures in the range of 20−60 °C, suggesting its further application as fluorometric temperature sensors. To the best of our knowledge, this work represents the first example of F^--reactive polymeric probes working in purely aqueous media, which are capable of highly sensitive and selective fluorescent F^- sensing in the form of both unimers and micellar nanoparticles.

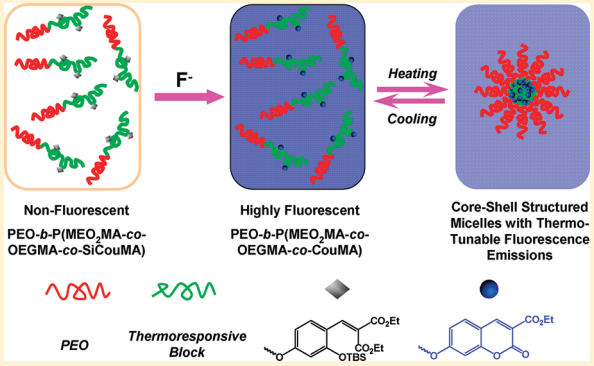

INTRODUCTION

The sensing and detection of fluoride ions (F^-) has aroused considerable interest in the past decade due to that F^- is highly relevant to health care, detection of nerve gases, and refinement of uranium resources.[1−5] For drinking water quality control, the EPA (United States Environmental Protection Agency) set a standard of 2−4 ppm to protect against osteofluorosis and dental fluorosis. However, for human beings of all ages, insufficient fluoride intake will incur increased risk of dental caries.[6] Therefore, it is highly important to develop selective, sensitive, fast, and cost-effective detection techniques for fluoride ions. Conventional analytical methods for F^- ions typically involve the use of ion chromatography,[7] ion-selective electrodes,[8,9] and capillary zone electrophoresis.[10] In addition, the optical detection of F^- ions has recently emerged to be the most convenient technique due to its simplicity, low cost, low detection limit, and suitability for detection at the intracellular and tissue-specific level. Moreover, concerning its practical applications, aqueous detection media is the best choice for optical F^- probes.

Up to now, three types of design strategies have been exploited to develop optical (colorimetric and/or fluorometric) probes of F^- ions, namely, supramolecular recognition,[11−25] Lewis acid−base interactions,[26−32] and F^- ion-induced chemical reactions.[33−45] Detection systems employing the former two strategies typically

Received: August 14, 2011
Revised: October 16, 2011
Published: October 25, 2011

Scheme 1. Schematic Illustration for the Fabrication Responsive Double Hydrophilic Block Copolymer- (DHBC-) Based Highly Selective and Sensitive Fluorescence Turn-On Probes for Fluoride Ions Working in Purely Aqueous Media by Exploiting F^--Induced Cyclization Reaction of Nonfluorescent Moieties To Induce the Formation of Fluorescent Coumarin Moieties within the Thermoresponsive Block

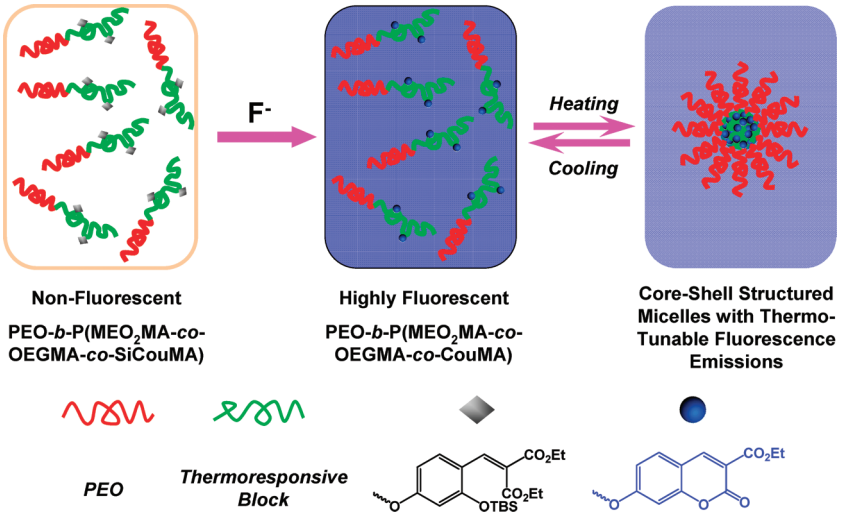

need to be conducted in organic solvents due to competitive interactions with water molecules, thus F^- sensing is only suitable for tetrabutylammonium salts and not quite applicable for the sodium or potassium salts; moreover, interference from the presence of $H_2PO_4^-$, AcO^-, and CN^- ions is unavoidable and the detection selectivity is a severe issue. To solve the selectivity problem, F^--induced chemical reactions such as the quite specific and selective Si−O bond cleavage have been utilized to design fluorescence "turn-on" reactive F^- sensors. Numerous fluorescent dyes such as coumarin,[37,40,46] fluorescein,[42] cyanine,[38] and 1,8-naphthalimide derivatives[35] were rendered nonfluorescent at first by caging with trialkylsilyoxy moiety, the presence of F^- ions can induce the deprotection of caging groups and turn-on the fluorescence emission. Quite recently, the construction of novel type of reactive fluorescence "turn-on" probes by employing F^- ion-induced direct cyclization reaction or the polymerization of nonfluorescent precursors into fluorescent species was also reported.[47,48]

Note that the above chemical reaction-based fluorometric F^- probes are exclusively based on small molecule dyes. In most cases, the measurements need to be conducted in purely organic solvents or less efficiently in organic solvent/water mixtures. This poses severe limitations to their biological applications such as bioassays at intracellular and tissue levels. Currently, there exist only two literature reports concerning small molecule-based fluorometric F^- probes in purely aqueous media.[38,49] Zhang et al.[38] reported the synthesis of *tert*- butyldiphenylsilyl caged dye bearing a quantized benzothiazolium moiety, which is water- soluble and can be applied for the intracellular fluorometric detection and imaging of fluoride ions. Yang et al.[49] constructed ratiometric fluorescent F^- probes on the basis of hydrophobic small molecule dyes embedded within surfactant micelle cores embedded, which can also work in aqueous media. Another notable disadvantage of small molecule reactive F^- probes is that they are difficult to be integrated with other analyte-sensing functions. Considering potential *in vivo* applications, they also possess inherent limits such as rapid elimination and extravasation out of the vasculature during blood circulation, which will restrict the timing for measurements.

We have recently been interested in the design of detection and sensing systems on the basis of responsive polymers and their assemblies.[50−54] The integration of responsive polymers with small molecule sensing motifs can allow for the construction of novel type of polymeric probes possessing multiple advantages such as excellent water solubility, multifunctional sensing capability, tunable detection sensitivity and selectivity, and enhanced biocompatibility. Concerning fluorescent polymeric probes for F^- ions, there exist only several relevant accounts. Tian et al.[55] reported that naphthalimide-functionalized poly(phenylacetylene) can serve as ratiometric fluorescent F^- probes in MeCN. We recently reported that secondary amine moieties in nitrobenzofurazan derivatives such as 4-(2-acryloyloxyethylamino)-7-nitro-2,1,3-benzoxadiazole (NBDAE) and NBDAE-containing polymers can serve as a new type of colorimetric and fluorometric F^- probes with a detection limit down to ∼0.8 μM.[56] Unimers and assembled micellar nanoparticles of coil−rod−coil ABA triblock copolymers consisting of a fluorescent conjugated polymer middle block and two outer NBDAE-containing coil blocks also exhibits ratiometric fluorescent sensing capability for F^- ions in acetone.[57]

The only example of polymeric fluorometric fluoride ion sensor exhibiting F^- ion-reactive characteristics was reported in 2003 by Swager and his co-workers.[58] They ingeniously incorporated newly designed chemical reaction-based F^- sensing moieties, which are initially nonfluorescent but subjected to spontaneous deprotection and subsequent structural rearrangement into highly fluorescent coumarin derivatives in the presence of F^- ions, into the side group of fluorescent conjugated polymer, polythiophene. Thus, F^- ion-induced generation of coumarin moieties in THF can effectively amplify the emission response via exciton migration from the conjugated backbone, resulting in ∼100-fold enhancement in F^- detection sensitivity for the modified conjugated polymer, as compared to the small molecule counterpart.[58,59]

It should be noted that all the above four examples of polymeric fluorescent F^- probes can only be applied in organic media. On the basis of the above analysis, it is highly desirable to

dx.doi.org/10.1021/ma2018588 |*Macromolecules* 2011, 44, 8780–8790

Scheme 2. Reaction Schemes Employed for the Synthesis of F^--Reactive Small Molecule Precursor (SiCou−OH, 7)

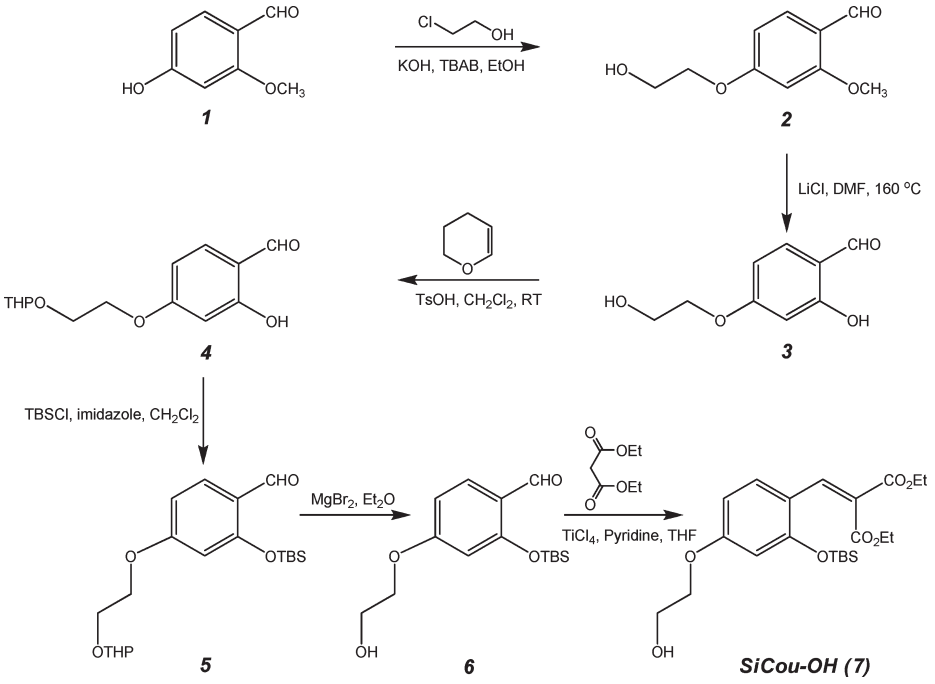

develop polymers or polymeric assemblies-based reactive fluorescence "turn-on" F^- probes that can effectively work in purely aqueous media. Herein, we report on the fabrication of a novel type of responsive double hydrophilic block copolymer- (DHBC-) based highly selective and sensitive fluorescence "turn-on" reactive probes for F^- ions working in aqueous media by utilizing F^--induced cyclization reaction of nonfluorescent moieties to induce the formation of fluorescent coumarin moieties (Scheme 1). It is worthy of noting that the F^- ion sensing structural motif was inspired by the previous work of Swager research group.[57] Diblock copolymers bearing F^--reactive moieties (SiCouMA) in the thermoresponsive block, PEO-*b*- P(MEO_2MA-*co*-OEGMA-*co*-SiCouMA), were synthesized at first (Schemes 2 and 3), where PEO, MEO_2MA, and OEGMA are poly(ethylene glycol), di(ethylene glycol) monomethyl ether methacrylate, and oligo(ethylene glycol) monomethyl ether methacrylate, respectively. The thermo-induced micellization of as-synthesized SiCouMA-labeled diblock copolymer, the F^--sensing capability including detection limits, sensitivity, and selectivity were explored in detail for both diblock unimers and micelles at temperatures below and above the critical micellization temperature (CMT).

EXPERIMENTAL SECTION

Materials. Poly(ethylene oxide) monomethyl ether (PEO_{113}−OH, M_n = 5.0 kDa, M_w/M_n = 1.06, mean degree of polymerization, DP, is 113) was purchased from Aldrich and used as received. Oligo(ethylene glycol) methyl ether methacrylate (OEGMA, M_n = 475, DP is 8−9; Aldrich) and di(ethylene glycol) methyl ether methacrylate (MEO_2MA, 95%, Aldrich) were passed through an alumina column to remove the inhibitor. All purified monomers were stored at −20 °C prior to use. 1,4-Dioxane, ethyl ether, and tetrahydrofuran (THF) were dried by refluxing over sodium/benzophenone and distilled prior to use. Dichloromethane (CH_2Cl_2), acetonitrile (MeCN), and pyridine were dried over CaH_2 and distilled just prior to use. 4-Hydroxy-2-methoxybenzaldehyde was recrystallized twice from deionized water and dried under reduced pressure. 2,2′-Azoisobutyronitrile (AIBN) was recrystallized from 95% ethanol. *N*,*N*′-Dicyclohexylcarbodiimide (DCC), 4-dimethylaminopyridine (DMAP), 2-chloroethanol, ethyl acetoacetate, acetic acid (AcOH), tetrabutylammonium bromide (TBAB), tetrabutylammonium fluoride (TBAF), lithium chloride (LiCl, anhydrous), 3,4-dihydro-2H-pyran (DHP), *tert*-butyldimethylsilyl chloride (TBSCl), 4- methylbenzenesulfonic acid (TsOH), diethyl malonate, ethyl acetate (EtOAc), and all other reagents were purchased from Sinopharm Chemical Reagent Co. Ltd. and used as received. Water was deionized with a Milli-Q SP reagent water system (Millipore) to a specific resistivity of 18.4 MΩ cm. 2-Succinyloxyethyl methacrylate (SEMA) was synthesized via the esterification reaction of 2-hydroxyethyl methacrylate (HEMA) with succinic anhydride according to literature procedures.[60] *S*-1-Propyl-*S*′-(α,α′-dimethyl-α″-acetic acid)- trithiocarbonate (PDMAT) and PEO_{113}-based macro-RAFT agent (PEO-CTA) were prepared via the esterification reaction of PEO_{113}−OH with PDMAT in the presence of DCC and DMAP.[51]

Sample Preparation. Synthetic schemes employed for the preparation of fluorescence "turn-on" small molecule precursor, diethyl 2-(2-((*tert*-butyldimethylsilyl)oxy)-4-(2- hydroxylethoxy)benzylidene)-malonate (SiCou−OH, **7**) and probe-functionalized double hydrophilic diblock copolymer, PEO-*b*-P(MEO_2MA-*co*-OEGMA-*co*-SiCouMA (**8**), are shown in Schemes 2 and 3, respectively.

*Synthesis of 4-(2-Hydroxyethoxy)-2-Methoxybenzaldehyde (**2**).* TBAB (0.64 g, 2 mmol), 4-hydroxy-2-methoxybenzaldehyde (**1**, 22.82 g, 0.15 mol), and NaOH (12.0 g, 0.30 mol) were dissolved in 300 mL absolute EtOH under nitrogen atmosphere. The reaction mixture was heated to reflux, and 2-chloroethanol (24.15 g, 0.30 mol) was added slowly via a dropping funnel within ∼1 h. After stirring overnight under reflux, the reaction mixture was allowed to cool to room temperature and filtered to remove precipitated salts. After evaporating all the solvents, the residues were dissolved in CH_2Cl_2, successively washed with 10% aqueous NaOH and water, dried over anhydrous $MgSO_4$, filtered, and then concentrated on a rotary evaporator. The crude product was subjected to

dx.doi.org/10.1021/ma2018588 |*Macromolecules* 2011, 44, 8780–8790

Scheme 3. Reaction Schemes Employed for the Synthesis of Double Hydrophilic Diblock Copolymers Bearing F^--Reactive Moieties (SiCouMA) within the Thermoresponsive Block, PEO-*b*-P(MEO_2MA-*co*-OEGMA-*co*-SiCouMA (8), via RAFT Polymerization[a]

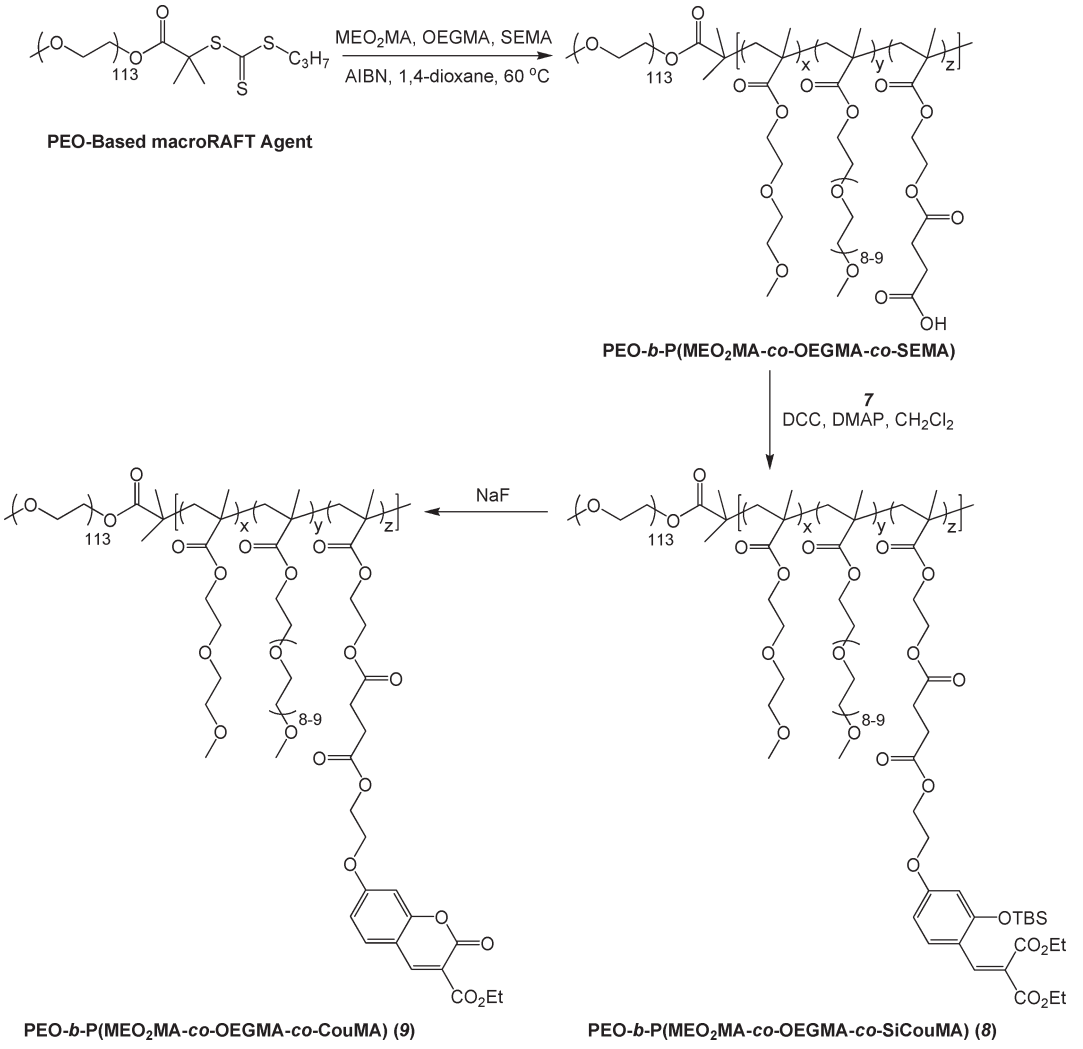

[a] In the presence of F^- ions, deprotection reaction followed by cyclization of SiCouMA moieties leads to the formation of highly fluorescent by employing PEO-*b*-P(MEO_2MA-*co*-OEGMA-*co*-CouMA) (**9**) bearing coumarin residues in the thermoresponsive block.

further purification by silica gel column chromatography using CH_2Cl_2 as the eluent, affording 4-(2-hydroxyethoxy)-2-methoxybenzaldehyde (**2**) as a yellowish solid (22.7 g, 77% yield). ^{1}H NMR ($CDCl_3$, δ, ppm, TMS): 10.27 (s, 1H, −C*H*O), 7.79, 6.54, and 6.48 (m, 3H, aromatic protons), 4.16 (t, 2H, −OCH$H_2$$CH_2$OH), 4.00 (t, 2H, −OCHH$_2CH_2$OH), 3.89 (s, 3H, −OC$H_3$), 1.74 (br, 1H, −OCHH$_2CH_2$O*H*).

*Synthesis of 4-(2-Hydroxyethoxy)salicylaldehyde (**3**).* A 500 mL round-bottom flask was charged with **2** (19.6 g, 0.10 mol), anhydrous LiCl (12.7 g, 0.30 mol), and DMF (200 mL). The mixture were heated to reflux under nitrogen atmosphere for 48 h, and then the reaction mixture was allowed to cool to room temperature, followed by the addition of 600 mL 10% aqueous NaOH. The solution pH was adjusted to ∼2. This was followed by extraction with EtOAc (100 mL × 3). The combined organic layers were washed with saturated brine, dried over anhydrous $MgSO_4$, filtered, and then concentrated on a rotary evaporator. The crude product was purified by silica gel column chromatography using CH_2Cl_2 as eluent, affording 4-(2-hydroxyethoxy)salicylaldehyde (**3**) as a white crystal (9.0 g, 49% yield). ^{1}H NMR ($CDCl_3$, δ, ppm, TMS; Figure S1, Supporting Information): 11.45 (s, 1H, Ar−O*H*), 9.72 (s, 1H, −C*H*O), 7.43, 6.56, and 6.43 (m, 3H, aromatic protons), 4.13 (t, 2H, −OCHH_2CH$_2$OH), 3.99 (t, 2H, −OCHH$_2$CH_2OH), 2.00 (br, 1H, −OCHH$_2$CH$_2$O*H*). ^{13}C NMR ($CDCl_3$, δ, ppm, TMS; Figure S1, Supporting Information): 194.63, 164.23, 155, 37, 135.31, 108.80, 101.42, 69.54, 64.64, 61.22.

*Synthesis of 2-Hydroxy-4-(2-((tetrahydro-2H-pyran-2-yl)oxy)ethoxy)-benzaldehyde (**4**).* To a stirred solution of **3** (3.64 g, 0.020 mol) and DHP (2.52 g, 0.030 mol) in CH_2Cl_2 (60 mL) at 25 °C, TsOH (20 mg, 0.12 mmol) was added and the reaction mixture was stirred for 2 h. The reaction mixture was washed with saturated aqueous NaCl solution (60 mL) for three times and dried with Na_2SO_4, and concentrated in vacuo. The residues obtained were subjected to flash column chromatography (silica gel, CH_2Cl_2) to afford 2-hydroxy-4-(2-((tetrahydro-2*H*-pyran-2-yl)oxy)ethoxy)benzaldehyde (**4**) as a yellow liquid (4.4 g, 83% yield). ^{1}H NMR ($CDCl_3$, δ, ppm, TMS; Figure S2, Supporting Information): 11.45 (s, 1H, Ar−O*H*), 9.72 (s, 1H, −C*H*O), 7.43, 6.56, and 6.43 (m, 3H, aromatic protons), 4.21 (m, 2H, −OCHH_2CH$_2$OTHP), 3.85 (m, 2H, −OCHH$_2$CH_2OTHP), 4.70, 3.53, 1.83, 1.74, 1.58 (m, 9H, −OTHP). ^{13}C NMR ($CDCl_3$, δ, ppm, TMS; Figure S2, Supporting Information): 194.16, 166.30, 164.58, 135.00, 115.07, 108.85, 101.45, 99.20, 67.82, 65.56, 62.14, 30.30, 25.16, 19.48.

dx.doi.org/10.1021/ma2018588 |*Macromolecules* 2011, 44, 8780–8790

*Synthesis of 2-((tert-Butyldimethylsilyl)oxy)-4-(2-((tetrahydro-2H-pyran-2-yl)oxy)ethoxy)benzaldehyde (**5**).* A 250 mL round-bottom flask was charged with **4** (2.66 g, 0.01 mol), imidazole (0.817 g, 0.012 mol), and anhydrous CH_2Cl_2 (100 mL), and then TBSCl (1.81 g, 0.012 mol) dissolved in 20 mL of anhydrous CH_2Cl_2 was slowly added dropwise over ~1 h. The reaction mixture was stirred at room temperature for 24 h. After that, the mixture was washed with saturated aqueous NaCl solution (100 mL) for three times, dried with anhydrous Na_2SO_4, and then concentrated in vacuo. The residues obtained were subjected to flash column chromatography (silica gel, CH_2Cl_2) to give 2-((*tert*-butyldimethylsilyl)oxy)-4-(2-((tetrahydro-2*H*-pyran-2-yl)oxy)ethoxy)-benzaldehyde (**5**) as a yellow liquid (3.5 g, 92% yield). ^{1}H NMR ($CDCl_3$, δ, ppm, TMS; Figure S3, Supporting Information): 10.28 (s, 1H, −C*H*O), 7.76, 6.60, 6.35 (m, 3H, aromatic protons), 4.17 (m, 2H, −OCH*H*$_2$CH$_2$OTHP), 3.84 (m, 2H, −OCHH$_2$C*H*$_2$OTHP), 4.68, 3.52, 1.81, 1.73, 1.56 (m, 9H, -OTHP), 1.00 (s, 6H, −OSi(C*H*$_3$)$_2$C-(CH$_3$)$_3$), 0.27 (s, 9H, −OSi(CH$_3$)$_2$C(C*H*$_3$)$_3$). ^{13}C NMR ($CDCl_3$, δ, ppm, TMS; Figure S3, Supporting Information): 188.39, 165.26, 160.58, 129.92, 121.20, 108.54, 105.60, 99.27, 67.97, 65.68, 62.19, 30.34, 25.66, 25.11, 19.33, 18.13, −4.45.

*Synthesis of 2-((tert-Butyldimethylsilyl)oxy)-4-(2-hydroxyethoxy)-benzaldehyde (**6**).* A 100 mL round-bottom flask was charged with **5** (2.28 g, 0.006 mol), $MgBr_2$ (3.32 g, 0.018 mol), and anhydrous ethyl ether (50 mL), and the reaction mixture was stirred at room temperature for 2 h and then washed with saturated aqueous NaCl solution (50 mL) three times. After drying with anhydrous Na_2SO_4 and removing all the solvents under reduced pressure, the residues obtained were subjected to flash column chromatography (silica gel, CH_2Cl_2) to give 2-((*tert*-butyldimethylsilyl)oxy)-4-(2-hydroxyethoxy)benzaldehyde (**6**) as a yellow liquid (1.5 g, 84% yield). ^{1}H NMR ($CDCl_3$, δ, ppm, TMS; Figure S4, Supporting Information): 10.30 (s, 1H, −CHO), 7.80, 6.59, 6.38 (m, 3H, aromatic protons), 4.11 (t, 2H, −OCH*H*$_2$CH$_2$OH), 3.99 (t, 2H, −OCHH$_2$C*H*$_2$OH), 1.96 (br, 1H, −OCHH$_2$CH$_2$O*H*), 1.02, (s, 6H, -OSi(C*H*$_3$)$_2$C(CH$_3$)$_3$), 0.29, (s, 9H, −OSi(CH$_3$)$_2$C(C*H*$_3$)$_3$). ^{13}C NMR ($CDCl_3$, δ, ppm, TMS; Figure S4, Supporting Information): 188.54, 164.49, 160.88, 130.36, 121.90, 108.11, 105.74, 69.71, 61.34, 25.31, 18.18, −4.07.

*Synthesis of Diethyl 2-(2-((tert-Butyldimethylsilyl)oxy)-4-(2-Hydroxyethoxy)benzylidene)malonate (**7**).* A 100 mL round-bottom flask was charged with 20 mL of anhydrous THF. After cooling to 0 °C in an ice−water bath, $TiCl_4$ (1.55 g, 0.008 mol) in 2 mL anhydrous CCl_4 was then added slowly at 0 °C. **6** (1.21 g, 0.004 mol) and diethyl malonate (0.65 g, 0.004 mol) in 5 mL of anhydrous THF was then added dropwise over ~0.5 h. Subsequently pyridine (1.32 g, 0.016 mol) in 2 mL of THF was added dropwise at 0 °C. The reaction mixture was stirred at 0 °C for another 0.5 h and then quenched with saturated aqueous NaCl solution and washed with saturated aqueous NaCl solution (50 mL) for three times. The combined organic phases were dried over anhydrous Na_2SO_4 and concentrated in vacuo. The residues obtained were subjected to flash column chromatography (silica gel, CH_2Cl_2) to afford 2-(2-((*tert*-butyldimethylsilyl)oxy)-4-(2-hydroxyethoxy)benzylidene)malonate (**7**) as a yellow liquid (1.2 g, 69% yield). ^{1}H NMR ($CDCl_3$, δ, ppm, TMS; Figure 1): 7.97, (s, 1H, Ar−C*H*C(COOCH$_2$CH$_3$)$_2$), 7.70, 6.60, 6.37, (m, 3H, aromatic protons), 4.29, (m, 4H, Ar−CHC(COOC*H*$_2$CH$_3$)$_2$), 4.11, (t, 2H, −OCH*H*$_2$CH$_2$OH), 3.99, (t, 2H, −OCHH$_2$C*H*$_2$OH), 1.96, (br, 1H, −OCHH$_2$CH$_2$O*H*), 1.30, (m, 6H, Ar−CHC(COOCH$_2$C*H*$_3$)$_2$), 1.00, (s, 9H, -OTBS), 0.29, (s, 9H, -OTBS). ^{13}C NMR ($CDCl_3$, δ, ppm, TMS; Figure 1): 167.30, 164.60, 161.80, 156.70, 137.42, 129.87, 118.14, 107.82, 106.16, 69.33, 61.37, 25.71, 18.26, 14.21, −4.31.

Synthesis of PEO-b-P(MEO$_2$MA-co-OEGMA-co-SEMA) Thermoresponsive Double Hydrophilic Diblock Copolymer. Typical procedures employed for the RAFT synthesis of thermoresponsive diblock copolymer, PEO-*b*-P(MEO$_2$MA-*co*-OEGMA-*co*-SEMA), are as follows. Into a reaction tube equipped with a magnetic stirring bar were charged

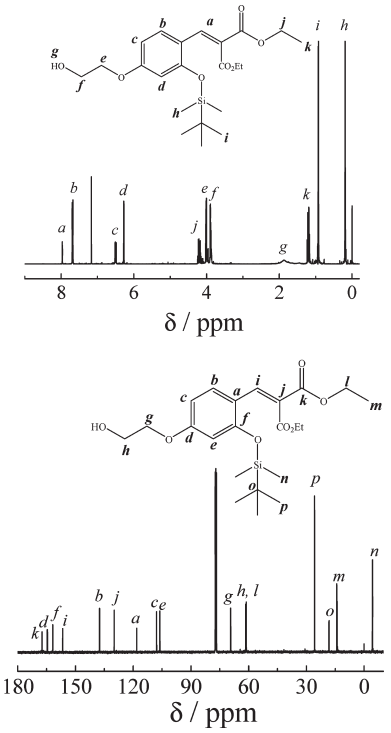

Figure 1. ^{1}H NMR and ^{13}C NMR spectra recorded in $CDCl_3$ for an F$^-$-reactive small molecule precursor (SiCou−OH, **7**).

MEO$_2$MA (2.71 g, 14.4 mmol), OEGMA (0.285 g, 0.60 mmol), SEMA (0.138 g, 0.60 mmol), PEO$_{113}$−CTA (0.783 g, 0.15 mmol), AIBN (0.006 g, 0.04 mol), and 1,4-dioxane (6 mL). The reaction tube was carefully degassed by three freeze−pump−thaw cycles and then sealed under vacuum. After thermostating at 60 °C in an oil bath and stirring for 10 h, the reaction tube was quenched into liquid nitrogen, opened, and diluted with 1,4-dioxane. The mixture was then precipitated into an excess of diethyl ether. The above dissolution−precipitation cycle was repeated for three times. PEO-*b*-P(MEO$_2$MA-*co*-OEGMA-*co*-SEMA) was obtained as a white solid (2.30 g, 58% yield). GPC analysis revealed an M_n of 23.3 kDa and an M_w/M_n of 1.15 (Figure S5, Supporting Information). The actual DP of P(MEO$_2$MA-*co*-OEGMA-*co*-SEMA) block (93), together with the molar contents of three comonomers were determined by ^{1}H NMR analysis. The final product was denoted as PEO$_{113}$-*b*-P(MEO$_2$MA$_{0.924}$-*co*-OEGMA$_{0.039}$-*co*-SEMA$_{0.037}$)$_{93}$.

*Synthesis of PEO-b-P(MEO$_2$MA-co-OEGMA-co-SiCouMA) (**8**).* The reactive probe- functionalized double hydrophilic diblock copolymer **8** was prepared by the postmodification of PEO$_{113}$-*b*-P(MEO$_2$MA$_{0.924}$-*co*-OEGMA$_{0.039}$-*co*-SEMA$_{0.037}$)$_{93}$ with **7** in the presence of DCC and DMAP. In a typical procedure, PEO$_{113}$-*b*-P(MEO$_2$MA$_{0.924}$-*co*-OEGMA$_{0.039}$-*co*- SEMA$_{0.037}$)$_{93}$ (1.20 g, 0.17 mmol carboxyl moieties) was dissolved in anhydrous toluene (10 mL), and then azeotropic distillation was carried out at 50 °C under reduced pressure to remove most of the solvent. **7** (0.011 g, 0.025 mmol) and dry CH_2Cl_2 (40 mL) were then added. After cooling to 0 °C in an ice−water bath, a mixture containing DCC (0.51 g, 0.25 mmol), DMAP (0.003 g, 0.025 mmol), and dry CH_2Cl_2 (10 mL) was added dropwise over ~1 h. The reaction mixture was stirred at room temperature for 24 h. After removing insoluble salts by filtration, the filtrates were concentrated on a rotary evaporator and then precipitated into an excess of cold diethyl ether. The above dissolution−precipitation cycle was repeated for three times. After drying in a vacuum oven overnight at room temperature, PEO-*b*-P(MEO$_2$MA-*co*-OEGMA-*co*- SiCouMA) (**8**) was obtained as a yellow solid (1.02 g, yield: 86%). The actual molar content of SiCouMA

dx.doi.org/10.1021/ma2018588 |*Macromolecules* 2011, 44, 8780–8790

residues in **8** was determined by UV−vis absorption spectroscopy in EtOH by using **7** as the calibration standard.

Characterization. All nuclear magnetic resonance (NMR) spectra were recorded on a Bruker AV300 NMR spectrometer (resonance frequency of 300 MHz for ^{1}H and 75 MHz for ^{13}C) operated in the Fourier transform mode. $CDCl_3$ was used as the solvent. Molecular weights and molecular weight distributions were determined by gel permeation chromatography (GPC) equipped with a Waters 1515 pump and a Waters 2414 differential refractive index detector (set at 30 °C). It used a series of two linear Styragel columns (HR2 and HR4) at an oven temperature of 45 °C. The eluent was THF at a flow rate of 1.0 mL/min. A series of low-polydispersity polystyrene standards were employed for calibration. All UV−vis spectra were acquired on a Unico UV/vis 2802PCS spectrophotometer. Concerning temperature-dependent turbidimetry, the optical transmittance of aqueous solutions at a wavelength of 600 nm was acquired on a Unico UV/vis 2802PCS spectrophotometer. A thermostatically controlled couvette was employed and the heating rate was 0.2 °C min^{-1}. The LCST was defined as the temperature corresponding to ∼1% decrease of optical transmittance. A commercial spectrometer (ALV/DLS/SLS-5022F) equipped with a multitau digital time correlator (ALV5000) and a cylindrical 22 mW UNIPHASE He−Ne laser (λ_0 = 632 nm) as the light source was employed for dynamic laser light scattering (LLS) measurements. Scattered light was collected at a fixed angle of 90° for duration of ∼10 min. Distribution averages and particle size distributions were computed using cumulants analysis and CONTIN routines. All data were averaged over three measurements. Fluorescence spectra were recorded using a RF-5301/PC (Shimadzu) spectrofluorometer. The temperature of the water-jacketed cell holder was controlled by a programmable circulation bath. The slit widths were set at 5 nm for excitation and 5 nm for emission.

RESULTS AND DISCUSSION

Synthesis and Thermo-Induced Aggregation of PEO-*b*-P(MEO$_2$MA-*co*-OEGMA-*co*-SiCouMA) (8). PMEO$_2$MA homopolymers and its random copolymers with OEGMA (DP = 8−9) are well-known to be thermoresponsive in aqueous solution and possess lower critical solution temperatures (LCST), which are quite similar to that exhibited by poly(*N*-isopropylacrylamide) (PNIPAM) in aqueous solution.[61] In the current case, well-defined double hydrophilic diblock copolymer precursor bearing carboxyl moieties in the thermoresponsive block, PEO-*b*-P(MEO$_2$MA-*co*-OEGMA-*co*-SEMA), was synthesized at first via the RAFT copolymerization of MEO$_2$MA, OEGMA, and SEMA comonomers using PEO$_{113}$−CTA as the macro-RAFT agent. The controlled RAFT polymerization of methacrylates monomers such as MEO$_2$MA and OEGMA has been well-documented in literature reports.[61,62] Compared to that of PEO$_{113}$−CTA macro-RAFT agent, the GPC elution trace of PEO-*b*-P(MEO$_2$MA-*co*-OEGMA-*co*-SEMA) precursor clearly shifted to the higher molecular weight (MW) side. Moreover, the elution peak is relatively sharp and symmetric, exhibiting no tailing at the lower molecular weight side, suggesting the high initiating efficiency of PEO$_{113}$-based macro-RAFT agent. GPC analysis of the carboxyl-functionalized diblock precursor revealed an M_n of 23.3 kDa and an M_w/M_n of 1.15 (Figure S5, Supporting Information). The actual DP of P(MEO$_2$MA-*co*-OEGMA-*co*-SEMA) block was determined to be 93 based on ^{1}H NMR analysis in $CDCl_3$. ^{1}H NMR analysis also revealed that within the thermoresponsive P(MEO$_2$MA-*co*-OEGMA-*co*-SEMA) block, the molar fraction of three comonomers, MEO$_2$MA, OEGMA, and SEMA are 0.924, 0.039, and 0.037, respectively. Thus, the diblock precursor was denoted as PEO$_{113}$-*b*-P(MEO$_2$MA$_{0.924}$-*co*-OEGMA$_{0.039}$-*co*-SEMA$_{0.037}$)$_{93}$. On average, there exist ∼3.44 carboxyl functionalities per diblock copolymer chain.

On the basis of the overall design as depicted in Schemes 1−3, the key point in the current work is the efficient synthesis of F^- ion-reactive fluorescence "turn-on" small molecule building block, **7**, which possesses one hydroxyethyl functionality for the covalent attachment with carboxyl moieties within PEO$_{113}$-*b*-P(MEO$_2$MA$_{0.924}$-*co*-OEGMA$_{0.039}$-*co*-SEMA$_{0.037}$)$_{93}$. Most importantly, probe **7** contains *tert*-butyldimethylsilyl protected diethyl 2-(benzylidene)- malonate motif. As discussed in the introduction part, the chemical design of **7** was inspired by the work of Swager et al.[58] In the presence of F^- ions, **7** is subjected to desilylation reaction, accompanied by the release of substituted phenol moieties; this step was spontaneously followed by the cyclization reaction to form highly fluorescent coumarin derivative (see Schemes 1 and 3 for details). Using 4-hydroxy-2-methoxybenzaldehyde (***1***) as the starting material,**7** was synthesized via six steps with an overall yield of 16.7%. ^{1}H NMR and ^{13}C NMR spectra of key intermediates, **3**, **4**, **5**, and **6**, are shown in Figures S1, S2, S3, and S4, Supporting Information, respectively, together with the peak assignments. ^{1}H NMR and ^{13}C NMR spectra of the target compound, **7**, are shown in Figure 1. All resonance signals can be well-assigned and peak integral ratios confirmed the successful synthesis of **7**.

With the small molecule F^- ion-reactive probe **7** in hand, we then covalently attached **7** onto the thermoresponsive block of PEO$_{113}$-*b*-P(MEO$_2$MA$_{0.924}$-*co*-OEGMA$_{0.039}$-*co*- SEMA$_{0.037}$)$_{93}$ via esterification reaction of **7** with carboxyl moieties within the diblock copolymer precursor. To ensure complete consumption of **7** in the reaction mixture, the [hydroxyl]/[carboxyl] feed molar ratio was kept to be quite low (∼1/6.8). Note that it is also quite advantageous to keep the labeling content of **7** within the thermoresponsive block at a relatively low level. If the labeling density on the diblock chain is too high, undesirable partial fluorescence quenching among F^- ion-generated coumarin species might occur;[63] moreover, a high labeling content of **7** this will also incur considerable changes in the critical micellization temperature (CMT) of the thermoresponsive diblock copolymer. ^{1}H NMR spectrum of PEO-*b*-P(MEO$_2$MA-*co*-OEGMA-*co*-SiCouMA) (**8**) in $CDCl_3$ is shown in Figure S6, Supporting Information. The presence of resonance signals characteristic of SiCouMA residues can be clearly discerned. The labeling density of SiCouMA on the final product, PEO-*b*-P(MEO$_2$MA-*co*-OEGMA-*co*- SiCouMA) (**8**), was calculated based on UV−vis absorption by using **7** as the calibration standard. For polymer **8** in ethanol at a concentration of 0.5 g/L, the SiCouMA concentration is determined to be ∼5.3 μM.

The thermoresponsive micellization behavior of PEO-*b*-P(MEO$_2$MA-*co*-OEGMA-*co*- SiCouMA) (**8**) in aqueous solution was then investigated by temperature-dependent optical transmittance and dynamic LLS measurements. Note that SiCouMA moieties in **8** exhibit slight reactivity even in neutral aqueous media, which will be discussed in detail in subsequent sections. To avoid possible interference from this, all UV−vis and dynamic LLS measurements were immediately carried out when freshly prepared samples are ready. Figure 2a shows the temperature-dependent optical transmittance of **8** in aqueous solution (1.0 g/L). It was found that the optical transmittance remains almost constant at temperatures below 32 °C.[61] Above 33 °C, the optical transmittance exhibits abrupt decrease, accompanied by the appearance of a bluish tinge, which is characteristic

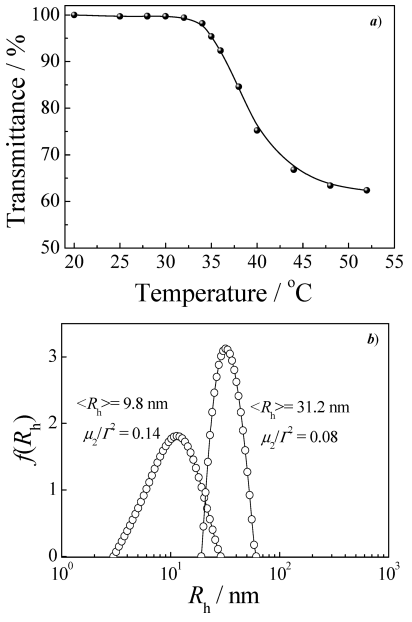

Figure 2. (a) Temperature dependence of optical transmittance at a wavelength of 600 nm recorded for 1.0 g/L aqueous solution of PEO-*b*-P(MEO$_2$MA-*co*-OEGMA-*co*-SiCouMA) (**8**) bearing F^--reactive moieties within the thermoresponsive block. (b) Hydrodynamic radius distributions, $f(R_h)$, recorded for 0.1 g/L aqueous solution of **8** at 20 and 40 °C.

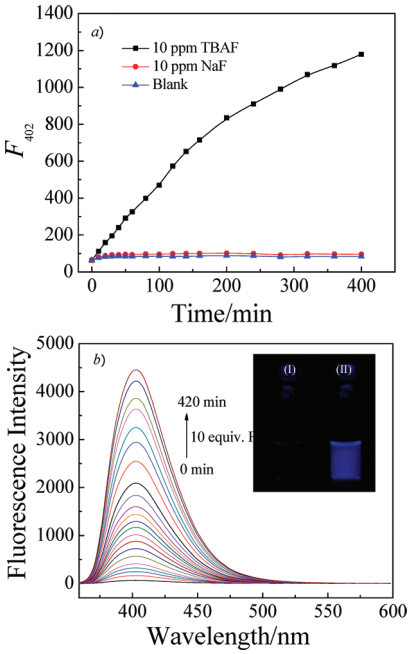

Figure 3. (a) Time-dependent changes in fluorescence emission intensities at 402 nm recorded for THF solution of **8** (0.5 g/L, 20 °C) upon addition of 100.0 equiv of TBAF and NaF, respectively. (b) Time-dependent evolution of fluorescence emission spectra recorded for the aqueous solution of PEO-*b*-P(MEO$_2$MA-*co*-OEGMA-*co*-SiCouMA) (**8**, 0.5 g/L, 5.3 μM SiCouMA moieties; 20 mM phosphate buffer; 20 °C) upon addition of 10.0 equiv. NaF (relative to SiCouMA moieties). The inset in (b) shows optical images recorded under UV 365 nm irradiation for aqueous solutions of **8** (0.5 g/L) (I) in the absence and (II) in the presence of NaF (10.0 equiv; 420 min after addition), respectively.

of colloidal dispersions. This suggests the occurrence of thermo-induced micellization due the thermoresponsiveness of P(MEO$_2$MA-*co*-OEGMA-*co*- SiCouMA) block. Thus, above the CMT of 33 °C, ***8*** will self-assemble into micellar nanoparticles possessing hydrophobic P(MEO$_2$MA-*co*-OEGMA-*co*-SiCouMA) cores stabilized by well-solvated PEO coronas (Scheme 1). The thermo-induced aggregation of **8** was further investigated by dynamic LLS. Figure 2b shows hydrodynamic radius distribution, $f(R_h)$, of **8** in aqueous solution (0.1 g/L) at 20 and 40 °C, respectively. At 20 °C, the intensity-average hydrodynamic radius, $\langle R_h \rangle$, is ~9.8 nm, suggesting that diblock copolymers exist as unimolecularly dissolved chains. Upon heating to 40 °C, the R_h distribution clearly shifts to higher values, affording an $\langle R_h \rangle$ of ~31.2 nm and a polydispersity, μ_2/Γ^2, of 0.08. This indicates that relatively monodisperse nanosized micellar nanoparticles were formed from PEO-*b*-P(MEO$_2$MA-*co*-OEGMA-*co*-SiCouMA) (**8**) at 40 °C, which is well above the CMT of diblock copolymers.

PEO-*b*-P(MEO$_2$MA-*co*-OEGMA-*co*-SiCouMA) Diblock Copolymer (8) Unimers and Micelles as Reactive Fluorescence "Turn-On" Probes for F^- Ions in Purely Aqueous Media. Previously, Swager et al.[58] covalently attached *tert*-butyldimethylsilyl protected diethyl 2-(benzylidene)malonate moiety (as contained in **7**, see Scheme 3) onto polythiophene conjugated polymers to achieve amplified fluorometric F^- ion detection. In THF solution, the addition TBAF leads to the deprotection of trialkylsilyl moieties and the subsequent generation of highly fluorescent coumarin side groups via cyclization. F^- ion-induced interconnection of the new transduction pathway to the fluorescent conjugated backbone resulted in ~100-fold enhancement of detection sensitivity. In the current work, we first investigated the F^- ion sensing capability of reactive PEO-*b*-P(MEO$_2$MA-*co*-OEGMA-*co*-SiCouMA) (**8**) in organic solvents, and the results are shown in Figure 3a. In the absence of TBAF, the emission intensity remains at constantly low background values, suggesting that SiCouMA residues in **8** is quite stable and no reaction have occurred. It was found that for 0.5 g/L THF solution of **8** (5.3 μM SiCouMA moieties) in the presence of 100.0 equiv of TBAF (final concentration 10.0 ppm), the emission intensity at 402 nm exhibit monotonic increase with the incubation time, suggesting the generation of coumarin moieties induced by fluoride ions. We can also observe that even at 400 min after the addition of TBAF, the emission intensity is still gradually increasing, suggesting that in THF, the reaction is quite slow. These preliminary results strongly suggest that ***8*** can act as a reactive fluorescence "turn-on" probe for TBAF.

Considering the poor bioavailability of organic TBAF salts and that most fluoride ions exist in the form sodium or potassium salts, next, we attempted to utilize the THF solution of **8** to detect NaF in a fluorometric manner. It is not strange that the addition of 100.0 equiv. NaF to **8** in THF essentially does not lead to any fluorescence emission enhancement, presumably due to the poor solubility of NaF in THF (Figure 3a). The addition of KF results in the same phenomenon as that of NaF. Since the detection, sensing, and imaging of F^- ions in drinking water and other biological samples (e.g., cells, tissues, and organs) are solely dealing with aqueous media, in the next section, we put emphasis on the fluorometric sensing of fluoride ions in purely aqueous media.

The general design principle is shown in Scheme 1. The covalent embedment of water-insoluble SiCouMA moieties into the thermoresponsive block of PEO-*b*-P(MEO$_2$MA- *co*-OEGMA-*co*-SiCouMA) (**8**) provides the advantage of much more

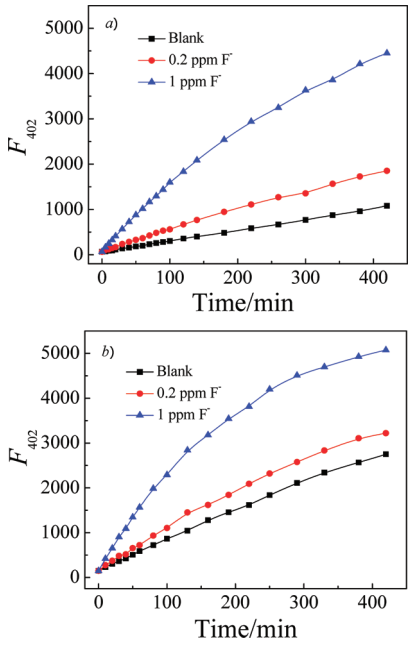

Figure 4. Time-dependent changes in fluorescence emission intensities at 402 nm recorded for the aqueous solution of **8** (0.5 g/L, 5.3 μM SiCouMA moieties; 20 mM phosphate buffer) at (a) 20 °C and (b) 40 °C upon addition of 2.0 and 10.0 equiv of NaF.

improved water solubility. Moreover, **8** can exist as unimers below the CMT and self-assemble into core−shell type micellar nanoparticle at elevated temperature due to the thermoresponsiveness of SiCouMA-labeled block. The formation of micelles can effectively encapsulate fluoride ion-reactive SiCouMA and F^--generated highly fluorescent CouMA within the hydrophobic cores, thus, multiple advantages such as the modulation of detection sensitivity, linear detection range, and possible integration of temperature detection capability are envisaged to be achieved.

We then monitored the time-evolution of fluorescence emission spectra recorded for the aqueous solution of **8** (0.5 g/L, pH 7.4) at 20 °C upon addition of 10.0 equiv of NaF (relative to SiCouMA moieties) and the results are shown in Figure 3b. Apparently, we can discern the prominent enhancement of emission at around 402 nm with the increase of incubation time. From the inset in Figure 3b, the presence of 10 equiv. (1.0 ppm) NaF clearly leads to the fluorometric transition from nonemissive to intense blue emission, which can be easily checked by the naked eye. Thus, at 20 °C, diblock unimers provides a facile detection approach for NaF. From Figure 4a, it can be quantified that the addition of 1.0 ppm (10.0 equiv) NaF leads to ∼69.2-fold increase in emission intensity in the time range of 0−420 min. In the presence of 0.2 ppm of NaF, ∼28.8-fold increase in the fluorescence intensity can be observed in the same time period. Moreover, the emission intensity−incubation time plot in the presence of 1.0 ppm of NaF possesses appreciably larger slope that in the presence of 0.2 ppm of NaF. This strongly suggests that diblock unimers of **8** can serve as reactive fluorescence "turn-on" probe for NaF in purely aqueous media.

Despite of the above positive results, we are quite conscious of the reactiveness of SiCouMA moieties in **8** toward water molecules even under neutral aqueous media (pH 7.4 buffer). The water reactivity of trialkylsilyl protecting groups has actually led to quite high background signal intensity for those trialkylsilyl-caged dyes due to competitive hydrolysis reactions by water molecules and by fluoride ions.[40−42,44,46] In the current design, the fluorescence "turn-on" involves two steps, namely, deprotection of *tert*-butyldimethylsilyl and cyclization reaction into the highly fluorescent coumarin moieties. As reported by Swager et al.,[58] in THF, the second step is the rate-determining one at F^- concentrations less than ∼3.0 equiv relative to that of SiCouMA residues. We suppose that this characteristic feature might be advantageous for the use of **8** as aqueous media-based fluorometric "turn-on" sensor for fluoride ions as the background emission intensity solely caused by spontaneous hydrolysis by water molecules can be retarded to some extent.

In the absence of NaF, the time evolution of emission intensity at 402 nm for **8** in aqueous media (pH 7.4) was then monitored at 20 and 40 °C for diblock unimers and micelles, respectively. As shown in parts a and b of Figure 4, emission intensities of the aqueous solution of **8** indeed exhibit slight increase with increasing incubation time duration. Diblock micelles at 40 °C exhibit more prominent increase with time compared to that 20 °C. However, we can clearly tell from Figure 4, parts a and b, that for diblock unimers and micelles at 20 and 40 °C, the presence of 0.2 and 1.0 ppm of NaF can both accelerate the fluorescence "turn-on" process, as evidenced by prominently elevated slopes of emission intensity-incubation time curves.

On the basis of the above results, we conclude that although the fluorescence intensity of the aqueous solution of **8** could be enhanced with increasing incubation time in the presence of NaF, extended duration of incubation will surely incur the increase of undesirable contribution by the water hydrolysis pathway. To effectively eliminate the premature fluorescence "turn-on" by the background aqueous media and to obtain reliable, consistent, and comparable analytical data, and to achieve fast fluoride ion detection, in subsequent sections, the incubation time was fixed to be 20 min after the addition of F^- ions.[43−46] During this time period, the background signal intensity incurred by water molecules can be kept at a minimum level.

For the aqueous solution of PEO-*b*-P(MEO_2MA-*co*-OEGMA-*co*-SiCouMA) (**8**) at a concentration of 0.5 g/L and 20 °C, the incubation time was fixed at 20 min after the addition of 0−1600 equiv of NaF (relative to SiCouMA residues), and the NaF concentration dependence of emission spectra are shown in Figure 5a. We can see that in the range of 0−1600 equiv of NaF, the emission intensity at 402 nm exhibits ∼88-fold increase. Most importantly, in the low NaF concentration range, there exists excellent linear relationship (R = 0.9989) between the emission intensity and NaF concentrations in the range of 0−15 ppm for diblock unimers at 20 °C with the coefficient (inset in Figure 5b).

At 40 °C, the diblock copolymer **8** spontaneously forms micellar nanoparticles. In the same NaF concentration range (0−1600 equiv), the emission intensity at 402 nm exhibits ∼30-fold enhancement compared to the blank sample (Figure 6). Moreover, the same linear relationship as observed for that of diblock unimers at 20 °C can be again obtained in the NaF concentration range of 0−8 ppm for diblock micelles at 40 °C (inset in Figure 6b). The ∼30-fold emission enhancement for diblock micelles at 40 °C is less potent than that at 20 °C for diblock unimers in the same range of NaF concentration (0−1600 equiv), this might be partially ascribed to the increase of background signal intensity incurred by the water hydrolysis pathway, as evidenced by the much faster increase of emission intensity with

dx.doi.org/10.1021/ma2018588 |*Macromolecules* 2011, 44, 8780–8790

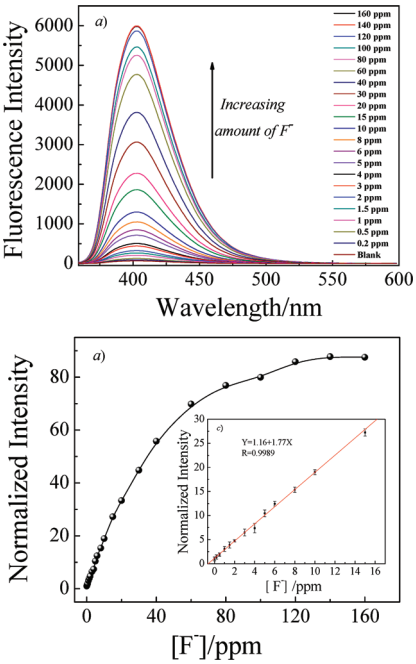

Figure 5. (a) Fluorescence emission spectra and (b) changes in relative fluorescence intensities at 402 nm recorded for the aqueous solution of PEO-*b*-P(MEO_2MA-*co*- OEGMA-*co*-SiCouMA) (***8***, 0.5 g/L, 5.3 μM SiCouMA moieties; 20 mM phosphate buffer; 20 °C) at 20 min after the addition of 0−1600 equiv. NaF. The inset (c) shows the enlarged region of part b in the range of 0−150 equiv (0−15 ppm) of NaF. All data points in parts b and c are averaged values from at least three parallel measurements.

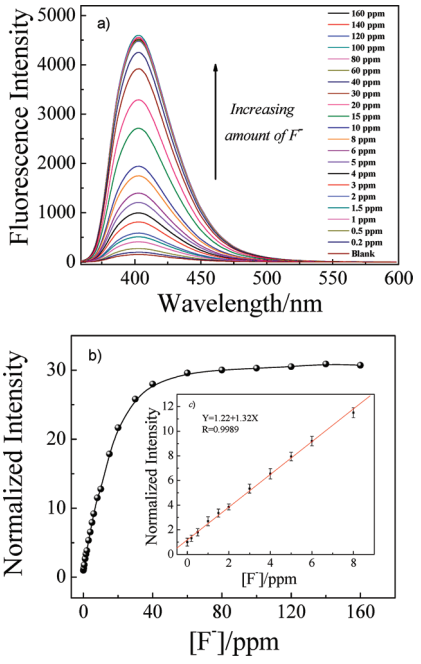

Figure 6. (a) Fluorescence emission spectra and (b) changes in relative fluorescence intensities at 402 nm recorded for the aqueous solution of PEO-*b*-P(MEO_2MA-*co*- OEGMA-*co*-SiCouMA) (***8***, 0.5 g/L, 5.3 μM SiCouMA moieties; 20 mM phosphate buffer; 40 °C) at 20 min after the addition of 0−1600 equiv of NaF. The inset (c) shows the enlarged region of part b in the range of 0−80 equiv (0−8 ppm) of NaF. All data points in parts b and c are averaged values from at least three parallel measurements.

incubation time for blank samples at 40 °C compared to that at 20 °C (Figure 4, parts a and b).

A direct comparison of results shown in Figure 6b with that in Figure 5b reveals that for diblock micelles at 40 °C, the addition of ~400 equiv of NaF can result in the complete consumption of SiCouMA moieties in ***8*** within just 20 min; whereas for diblock unimers at 20 °C, ~1200 equiv. NaF need to be added to achieve comparable conversion of reactive SiCouMA species. This implies that NaF detection using diblock micelles at 40 °C can achieve considerably faster response time. If we arbitrarily define the detection limit as the NaF concentration at which a 10% fluorescence enhancement can be measured by employing 0.5 g/L aqueous solution of **8**, the detection limit toward F^- ions was determined to be ~0.065 ppm at 20 °C for diblock unimers; for diblock micelles at 40 °C, the detection limit is slightly improved to ~0.05 ppm (Figure 7, parts a and b). Considering the practical application of F^- ion sensing in drinking water or relevant biological media, fluorescence emission spectra and changes in relative intensities at 402 nm were also recorded for the micellar solution of **8** at 37 °C (Figure S7, Supporting Information). It was found that the fluorometric F^- ion-sensing performance is quite comparable to that occurred at 40 °C (Figure 6), with the detection limit being ~0.053 ppm.

A closer examination of Figures 5a and 6a revealed that upon complete reaction of SiCouMA species of **8**, diblock unimer solutions at 20 °C exhibit higher emission intensities than that for diblock micelles at 40 °C. To further probe this, the temperature-dependent fluorescence emission spectra were collected for **8** in aqueous solution subjected to complete SiCouMA reaction (1600 equiv., overnight). We observe the prominent decrease of emission intensity with increasing temperature (Figure S8a, Supporting Information). Most importantly, an almost linear relationship (R = 0.997) between the relative fluorescence intensity (I/I_0) and temperature was obtained in the range of 20−60 °C (Figure S8b, Supporting Information). The same phenomenon has been previously observed for coumarin-functionalized poly(vinyl alcohol).[64] On the basis of these results, PEO-*b*-P(MEO_2MA-*co*-OEGMA-*co*-SiCouMA) (**8**) is also endowed with the fluorometric temperature sensing function, in addition to serving as a highly sensitive chemical reaction-based fluorescence "turn-on" probe for fluoride ions in purely aqueous media.

Finally, the detection selectivity of ***8*** for fluoride ions was examined. At a polymer concentration of 0.5 g/L, 100 equiv of sodium salts of Cl^-, Br^-, I^-, CO_3^{2-}, NO_3^-, HSO_4^-, HPO_4^{2-}, $H_2PO_4^-$, AcO^-, and F^- were added, respectively. It was observed that 20 min after addition, only F^- ions exhibit prominent fluorescence emission enhancement, and no other ions induce discernible changes in emission intensities (Figure 8). This clearly verified the high selectivity of diblock copolymer **8** as a chemical reaction-based fluorescence "turn-on" probe for fluoride ions in aqueous media.

On the basis of the above results, we expect that the fluorometric sensing of F^- ions by PEO-*b*-P(MEO_2MA-*co*-OEGMA-*co*-SiCouMA) unimers and micelles in purely aqueous media should be applicable in practical circumstances such as drinking water analysis and cell or tissue-based assays in biological media. In the latter case, mildly acidic pH condition (e.g., intracellular microenvironment: pH ~5−6 for endosomes and lysosomes) might be encountered. However, it is well-known that the silyl ether moiety in SiCouMA is less stable and subjected to

dx.doi.org/10.1021/ma2018588 |*Macromolecules* 2011, 44, 8780–8790

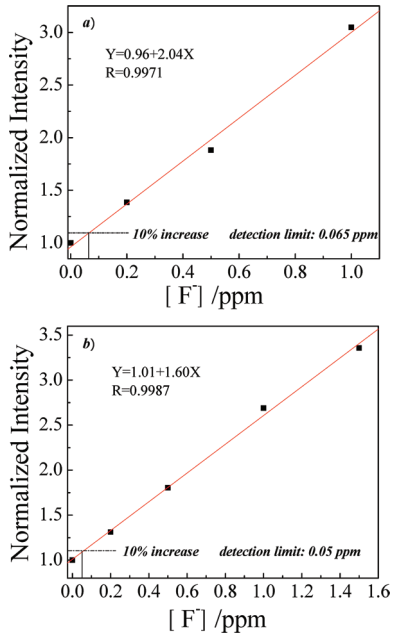

Figure 7. Determination of F^- detection limits for 0.5 g/L aqueous solution of PEO-*b*- P(MEO_2MA-*co*-OEGMA-*co*-SiCouMA) (**8**, 5.3 μM SiCouMA moieties; 20 mM phosphate buffer) at (a) 20 and (b) 40 °C, respectively.

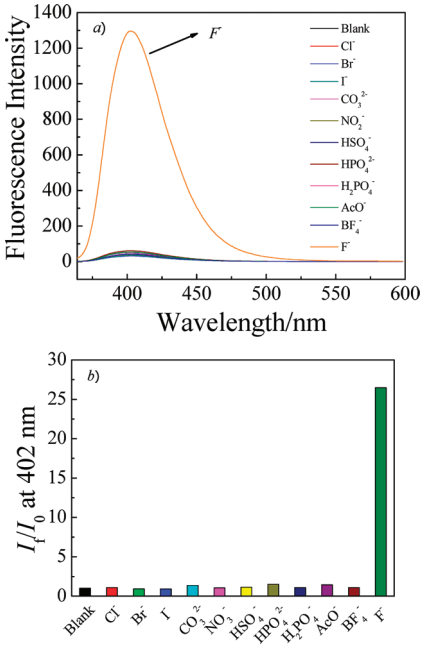

Figure 8. (a) Fluorescence emission spectra and (b) relative fluorescence emission intensities at 402 nm recorded for 0.5 g/L aqueous solution (20 °C) of PEO-*b*-P(MEO_2MA-*co*-OEGMA-*co*-SiCouMA) at ~20 min after the addition of 100 equiv of Cl^-, Br^-, I^-, CO_3^{2-}, NO_3^-, HSO_4^-, HPO_4^{2-}, $H_2PO_4^-$, AcO^-, and F^- ions (sodium salts in all cases), respectively.

hydrolysis reaction in acidic media, which is especially fast at low pH. To further probe the scope of applications, we also examined the stability of PEO-*b*-P(MEO_2MA-*co*-OEGMA- *co*-SiCouMA) copolymer at pH 5.0 and the results are shown in Figure S9, Supporting Information. It was found that the time-dependent profile of emission intensity changes at pH 5.0 is quite comparable to those occurred at pH 7.0. After 1 h incubation in the absence of F^- ions, ~3.3-fold and 3.1-fold increase in emission intensities were observed at pH 5.0 and pH 7.4, respectively. We also found that at pH 3.0, the hydrolysis reaction is much faster, exhibiting ~10.7-fold emission intensity increase after incubation for duration of 1 h. Thus, for strongly acidic aqueous samples (pH < 5), though less frequently associated with bioassay conditions, the preadjusting of solution pH to >5.0 is quite preferred. Another issue is the thermal stability of SiCouMA moieties on PEO-*b*-P(MEO_2MA-*co*-OEGMA-*co*-SiCouMA). We attempted to heat the THF solution of diblock copolymer to 50 °C and monitored the evolution of emission intensities at 402 nm (Figure S10, Supporting Information). It was found that within ~400 min upon heating, the emission intensity remains essentially constant, suggesting that SiCouMA moieties on the diblock copolymer are structurally stable at elevated temperatures. Note that the slight increase in emission intensity occurred initially should be ascribed to the presence of residual water traces in THF.

CONCLUSIONS

In summary, we report on the fabrication of a novel type of responsive double hydrophilic block copolymer (DHBC)-based highly selective and sensitive fluorescence "turn-on" reactive probes for fluoride ions (F^-) working in purely aqueous media by exploiting F^--induced cyclization reaction of nonfluorescent moieties to induce the formation of fluorescent coumarin moieties within the thermoresponsive block. Diblock copolymers bearing F^--reactive moieties (SiCouMA) in the thermoresponsive block, PEO-*b*-P(MEO_2MA-*co*-OEGMA-*co*-SiCouMA), were synthesized, which molecularly dissolve in water at room temperature and self-assemble into micellar nanoparticles above the critical micellization temperature (CMT, 33 °C). In the presence of F^- ions, deprotection of nonfluorescent SiCouMA moieties followed by spontaneous cyclization reaction leads to the formation of highly fluorescent coumarin residues (CouMA). Thus, PEO-*b*-P(MEO_2MA-*co*-OEGMA-*co*-SiCouMA) diblock copolymers can serve as highly efficient and selective fluorescence "turn-on" reaction probes for F^- ions in aqueous media. In the range of 0−1600 equiv of F^- ions, diblock unimers and micellar solutions at 20 and 40 °C exhibit ~88-fold and ~30-fold increase in fluorescence emission intensity (20 min incubation time), respectively. The detection limits were determined to be 0.065 and 0.05 ppm for diblock unimers and micelles, respectively. Upon complete transformation of nonfluorescent SiCouMA moieties into fluorescent CouMA, the emission intensity of diblock copolymer solution decreases linearly with temperatures in the range of 20−60 °C, suggesting its further application as fluorometric temperature sensors.

To the best of our knowledge, this work represents the first example of F^--reactive polymeric probes working in purely aqueous media, which are capable of highly sensitive and selective fluorescent F^- sensing in the form of both unimers and micellar nanoparticles. We demonstrate that the combination of stimuli-responsive block copolymers with chemical reaction-based small molecule fluorescent sensing motifs can offer combined advantages such as water dispersibility, biocompatibility, and the capability of integration with temperature sensing functions. One drawback of the current system is that calibration curves

need to be established prior to sample measurements, partially due to that the fluorometric sensing is based on intensity changes of a single emission band. Further works including the fabrication of responsive polymer-based ratiometric fluorescent F^- probes are currently underway.

■ ASSOCIATED CONTENT

Supporting Information. Characterization data of ^1H NMR, ^{13}C NMR, GPC, and additional fluorescence spectrometry results. This material is available free of charge via the Internet at http://pubs.acs.org.

■ AUTHOR INFORMATION

Corresponding Author
*E-mail: (S.L.) sliu@ustc.edu.cn; (H.Z.) huizhong@hytc.edu.cn.

■ ACKNOWLEDGMENT

The financial support from National Natural Scientific Foundation of China (NNSFC) Projects (20874092, 91027026, 20975043, and 51033005) and Fundamental Research Funds for the Central Universities is gratefully acknowledged.

■ REFERENCES

(1) Beer, P. D.; Gale, P. A. *Angew. Chem., Int. Ed.* **2001**, *40*, 486–516.
(2) Kostyuk, P. G.; Krishtal, O. A.; Pidoplichko, V. I. *Nature* **1975**, *257*, 691–693.
(3) Kubik, S. *Chem. Soc. Rev.* **2009**, *38*, 585–605.
(4) Langmuir, D. *Geochim. Cosmochim. Acta* **1978**, *42*, 547–569.
(5) Schmidtchen, F. P.; Berger, M. *Chem. Rev.* **1997**, *97*, 1609–1646.
(6) Kirk, K. L. *Biochemistyr of the Halogens and Inorganic Halides*; Plenum Press: New York, 1991; p58.
(7) Katruzov, A. N.; Nikitina, T. G.; Moskvin, L. N. *J. Anal. Chem.* **1998**, *53*, 173–177.
(8) Frant, M. S.; Ross, J. W. *Science* **1966**, *154*, 1553–&.
(9) Hara, H.; Huang, C. C. *Anal. Chim. Acta* **1997**, *338*, 141–147.
(10) Bodor, R.; Madajova, V.; Masar, M.; Johnck, M.; Stanislawski, B.; Kaniansky, D. *J. Chromatogra. A* **2001**, *916*, 155–165.
(11) Cametti, M.; Rissanen, K. *Chem. Commun.* **2009**, 2809–2829.
(12) Boiocchi, M.; Del Boca, L.; Gomez, D. E.; Fabbrizzi, L.; Licchelli, M.; Monzani, E. *J. Am. Chem. Soc.* **2004**, *126*, 16507–16514.
(13) Esteban-Gomez, D.; Liechelli, M.; Fabbrizzi, L. *J. Org. Chem.* **2005**, *70*, 5717–5720.
(14) Kruger, P. E.; Jensen, P.; Pfeffer, F. M.; Hussey, G. M.; Gunnlaugsson, T. *Tetrahedron Lett.* **2003**, *44*, 8909–8913.
(15) Qu, Y.; Hua, J. L.; Tian, H. *Org. Lett.* **2010**, *12*, 3320–3323.
(16) Bok, J. H.; Bartsch, R. A.; Lee, J. Y.; Kim, J. S.; Kim, S. K. *Org. Lett.* **2005**, *7*, 4839–4842.
(17) Liu, B.; Tian, H. *J. Mater. Chem.* **2005**, *15*, 2681–2686.
(18) Cho, E. J.; Moon, J. W.; Ko, S. W.; Lee, J. Y.; Kim, S. K.; Yoon, J.; Nam, K. C. *J. Am. Chem. Soc.* **2003**, *125*, 12376–12377.
(19) Mizuno, T.; Wei, W. H.; Eller, L. R.; Sessler, J. L. *J. Am. Chem. Soc.* **2002**, *124*, 1134–1135.
(20) Peng, X. J.; Wu, Y. K.; Fan, J. L.; Tian, M. Z.; Han, K. L. *J. Org. Chem.* **2005**, *70*, 10524–10531.
(21) He, X. M.; Hu, S. Z.; Liu, K.; Guo, Y.; Xu, J.; Shao, S. J. *Org. Lett.* **2006**, *8*, 333–336.
(22) Wang, Q. G.; Ding, Y. B.; Li, X.; Zhu, W. H.; Xie, Y. S. *Chem. Commun.* **2010**, *46*, 3669–3671.
(23) He, X. M.; Yam, V. W. W. *Org. Lett.* **2011**, *13*, 2172–2175.
(24) Yang, Z. P.; Zhang, K.; Gong, F. B.; Li, S. Y.; Chen, J.; Ma, J. S.; Sobenina, L. N.; Mikhaleva, A. I.; Trofimov, B. A.; Yang, G. Q. *J. Photochem. Photobiol. A—Chem.* **2011**, *217*, 29–34.
(25) Kim, S. K.; Yoon, J. *Chem. Commun.* **2002**, 770–771.
(26) Arimori, S.; Fyles, T. M.; Hibbert, T. G.; James, T. D.; Kociok-Kohn, G. I.; Davidson, M. G. *Chem. Commun.* **2004**, 1640–1641.
(27) Saxena, A.; Fujiki, M.; Rai, R.; Kim, S. Y.; Kwak, G. *Macromol. Rapid Commun.* **2004**, *25*, 1771–1775.
(28) Melaimi, M.; Gabbai, F. P. *J. Am. Chem. Soc.* **2005**, *127*, 9680–9681.
(29) Xu, S.; Chen, K. C.; Tian, H. *J. Mater. Chem.* **2005**, *15*, 2676–2680.
(30) Hudson, Z. M.; Wang, S. N. *Acc. Chem. Res.* **2009**, *42*, 1584–1596.
(31) Liu, X. Y.; Bai, D. R.; Wang, S. N. *Angew. Chem., Int. Ed.* **2006**, *45*, 5475–5478.
(32) Shirasaka, T.; Akiyama, S.; Tamao, K.; Yamaguchi, S. *J. Am. Chem. Soc.* **2002**, *124*, 8816–8817.
(33) Bozdemir, O. A.; Sozmen, F.; Buyukcakir, O.; Guliyev, R.; Cakmak, Y.; Akkaya, E. U. *Org. Lett.* **2010**, *12*, 1400–1403.
(34) Bhalla, V.; Singh, H.; Kumar, M. *Org. Lett.* **2010**, *12*, 628–631.
(35) Zhang, J. F.; Lim, C. S.; Bhuniya, S.; Cho, B. R.; Kim, J. S. *Org. Lett.* **2011**, *13*, 1190–1193.
(36) Kim, S. Y.; Hong, J. I. *Org. Lett.* **2007**, *9*, 3109–3112.
(37) Sokkalingam, P.; Lee, C. H. *J. Org. Chem.* **2011**, *76*, 3820–3828.
(38) Zhu, B. C.; Yuan, F.; Li, R. X.; Li, Y. M.; Wei, Q.; Ma, Z. M.; Du, B.; Zhang, X. L. *Chem. Commun.* **2011**, *47*, 7098–7100.
(39) Baker, M. S.; Phillips, S. T. *J. Am. Chem. Soc.* **2011**, *133*, 5170–5173.
(40) Yang, X. F. *Spectrochim. Acta A* **2007**, *67*, 321–326.
(41) Yang, X. F.; Qi, H. P.; Wang, L. P.; Su, Z.; Wang, G. *Talanta* **2009**, *80*, 92–97.
(42) Yang, X. F.; Ye, S. J.; Bai, Q.; Wang, X. Q. *J. Fluoresc.* **2007**, *17*, 81–87.
(43) Li, Y. M.; Zhang, X. L.; Zhu, B. C.; Yan, J. L.; Xu, W. P. *Anal. Sci.* **2010**, *26*, 1077–1080.
(44) Zhu, C. Q.; Chen, J. L.; Zheng, H.; Wu, Y. Q.; Xu, J. G. *Anal. Chim. Acta* **2005**, *539*, 311–316.
(45) Hu, R.; Feng, J. A.; Hu, D. H.; Wang, S. Q.; Li, S. Y.; Li, Y.; Yang, G. Q. *Angew. Chem., Int. Ed.* **2010**, *49*, 4915–4918.
(46) Kim, S. Y.; Park, J.; Koh, M.; Park, S. B.; Hong, J. I. *Chem. Commun.* **2009**, 4735–4737.
(47) Li, G.; Gong, W. T.; Ye, J. W.; Lin, Y. A.; Ning, G. L. *Tetrahedron Lett.* **2011**, *52*, 1313–1316.
(48) Padie, C.; Zeitler, K. *New J. Chem.* **2011**, *35*, 994–997.
(49) Hu, R.; Feng, J. A.; Hu, D. H.; Wang, S. Q.; Li, Y.; Yang, G. Q. *Angew. Chem., Int. Ed.* **2010**, *49*, 4915–4918.
(50) Liu, T.; Liu, S. Y. *Anal. Chem.* **2011**, *83*, 2775–2785.
(51) Hu, J. M.; Li, C. H.; Liu, S. Y. *Langmuir* **2010**, *26*, 724–729.
(52) Hu, J. M.; Liu, S. Y. *Macromolecules* **2010**, *43*, 8315–8330.
(53) Yoon, J.; Kim, H. N.; Guo, Z. Q.; Zhu, W. H.; Tian, H. *Chem. Soc. Rev.* **2011**, *40*, 79–93.
(54) Yin, J.; Hu, H. B.; Wu, Y. H.; Liu, S. Y. *Polym. Chem.* **2011**, *2*, 363–371.
(55) Qu, Y.; Hua, J. L.; Jiang, Y. H.; Tian, H. *J. Polym. Sci., Part A: Polym. Chem.* **2009**, *47*, 1544–1552.
(56) Hu, J. M.; Li, C. H.; Cui, Y.; Liu, S. Y. *Macromol. Rapid Commun.* **2011**, *32*, 610–615.
(57) Hu, J. M.; Zhang, G. Y.; Geng, Y. H.; Liu, S. Y. *Macromolecules* **2011**, DOI: 10.1021/ma201777p.
(58) Kim, T. H.; Swager, T. M. *Angew. Chem., Int. Ed.* **2003**, *42*, 4803–4806.
(59) Thomas, S. W.; Joly, G. D.; Swager, T. M. *Chem. Rev.* **2007**, *107*, 1339–1386.
(60) Cai, Y. L.; Armes, S. P. *Macromolecules* **2005**, *38*, 271–279.
(61) Hoth, A.; Lutz, J. F. *Macromolecules* **2006**, *39*, 893–896.
(62) Han, S.; Ishizone, T.; Hagiwara, M. *Macromolecules* **2003**, *36*, 8312–8319.
(63) Amir, R. J.; Albertazzi, L.; Willis, J.; Khan, A.; Kang, T.; Hawker, C. J. *Angew. Chem., Int. Ed.* **2011**, *50*, 3425–3429.
(64) Wang, B. Y.; Guan, X. L.; Hu, Y. L.; Su, Z. X. *Polym. Adv. Technol.* **2007**, *18*, 529–534.